

1 Increased hurricane frequency near Florida during Younger
2 Dryas Atlantic Meridional Overturning Circulation
3 slowdown

4 Michael R. Toomey^{1,2}, Robert L. Korty³, Jeffrey P. Donnelly², Peter J. van
5 Hengstum⁴, and William B. Curry⁵

6 *¹Eastern Geology and Paleoclimate Science Center, U.S. Geological Survey, Reston,
7 Virginia 20192, USA*

8 *²Department of Geology & Geophysics, Woods Hole Oceanographic Institution, Woods
9 Hole, Massachusetts 02543, USA*

10 *³Department of Atmospheric Sciences, Texas A&M University, College Station, Texas
11 77843, USA*

12 *⁴Department of Marine Sciences, Texas A&M University at Galveston, Galveston, Texas
13 77554, USA*

14 *⁵Bermuda Institute of Ocean Sciences, St. George's GE 01, Bermuda*

15 **ABSTRACT**

16 The risk posed by intensification of North Atlantic hurricane activity remains
17 controversial, in part due to a lack of available storm proxy records that extend beyond
18 the relatively stable climates of the late Holocene. Here we present a record of storm-
19 triggered turbidite deposition offshore the Dry Tortugas, south Florida, USA, that spans
20 abrupt transitions in North Atlantic sea-surface temperature and Atlantic Meridional
21 Overturning Circulation (AMOC) during the Younger Dryas (12.9–11.7 k.y. B.P.).
22 Despite potentially hostile conditions for cyclogenesis in the tropical North Atlantic at

23 this time, our record and numerical experiments suggest that strong hurricanes may have
24 regularly impacted Florida. Less severe surface cooling at mid-latitudes ($\sim 20\text{--}40^\circ\text{N}$) than
25 across much of the tropical North Atlantic ($\sim 10\text{--}20^\circ\text{N}$) in response to AMOC reduction
26 may best explain strong hurricane activity during the Younger Dryas near the Dry
27 Tortugas and, potentially, along the entire southeastern coast of the United States.

28 **INTRODUCTION**

29 Reduction in Atlantic Meridional Overturning Circulation (AMOC) during the
30 Younger Dryas (YD), most often attributed to meltwater release during drainage of
31 glacial Lake Agassiz (e.g., Clark et al., 2001 and refs. therein), may have lowered sea-
32 surface temperatures (SSTs) in the North Atlantic (e.g. Schmidt and Lynch-Stieglitz,
33 2011) and therefore, the potential intensity of tropical cyclones (TCs). However, the
34 environmental controls on TC activity (genesis, track, intensity) are complex, responding
35 not only to changes in local SST but also vertical wind shear and humidity. For instance,
36 Kerty et al. (2012) showed a globally heterogeneous response of TC activity to
37 universally colder temperatures in PMIP2 (<http://pmip2.lscce.ipsl.fr/>) simulations of the
38 Last Glacial Maximum (21 k.y. B.P.). Future, multi-model mean (CMIP5, [http://cmip-
39 pcmdi.llnl.gov/index.html](http://cmip-pcmdi.llnl.gov/index.html)), projections, assuming a high emissions scenario, anticipate
40 increased TC potential intensity across much of the tropical North Atlantic by the end of
41 this century (Sobel et al., 2016), but it remains unclear if this would translate into more
42 landfalling intense hurricanes along the basin margins. Historic observations (1947–2015
43 CE) demonstrate that warm SSTs and low vertical wind shear in the Main Development
44 Region (MDR) (Fig. 1A) have often fostered increased basin-wide TC activity while
45 coinciding with less favorable conditions for storm intensification along the Eastern

46 Seaboard (Kossin, 2017). No proxy records or comparable modeling experiments of TC
47 activity currently exist for the YD that could be used to test if severe changes in MDR
48 thermodynamic structure, likely to impact cyclone intensity, were counter-balanced by
49 more favorable conditions elsewhere in the basin.

50 Proxy-based reconstruction of past TC activity using coarse-grained overwash
51 deposits in lower energy back-barrier marshes or lagoons (e.g., Donnelly et al., 2001) has
52 typically been limited to the mid-late Holocene (typically < 5 k.y. B.P.) due to shoreward
53 transgression of these environs in response to deglacial sea-level rise (Bard et al., 2010).
54 However, re-suspension of sediment on continental shelves by storm-induced currents, its
55 subsequent transport offshore and deposition within margin sedimentary sequences could
56 potentially yield much longer records of past TC landfalls. Shanmugam (2008) reviewed
57 observations from modern storms which document bottom water velocities regularly in
58 excess of 1 m s^{-1} on continental shelves and offshore sediment transport. Toomey et al.
59 (2013) found that deposition of coarse-grained layers in an offbank transect of multi-
60 cores (~200–500 m below sea level [mbsl]) from the Bahamas (Fig. 1B) closely tracked
61 the passage of 10 major hurricanes between ~1915 and 1965 CE. Older deposits at that
62 site, thought to reflect increased mid-late Holocene hurricane activity, are consistent with
63 published Caribbean back-barrier overwash records (Toomey et al., 2013 and refs.
64 therein).

65 Here we use jumbo piston cores (JPCs) from offshore the Dry Tortugas, Florida,
66 that span the YD and early Holocene (EH) (Lynch-Stieglitz et al., 2011), to extend the
67 Bahamas paleo-hurricane reconstruction of Toomey et al. (2013) (located ~400 km east).
68 Florida is in the path of storms tracking out of the eastern Atlantic, western Caribbean

69 and Gulf of Mexico; sedimentary archives there are well positioned to capture changes in
70 North Atlantic cyclogenesis. Together with analysis of general circulation model (GCM)
71 experiments, we address two main questions: (1) how do cooler SSTs and/or AMOC
72 slowdown impact North Atlantic TC activity? (2) Are model-simulated changes in
73 storminess consistent with our proxy-based record of TC landfalls near Florida?

74 **MATERIALS AND METHODS**

75 The Florida margin (Fig. 1) near the Dry Tortugas Islands (25°N, 83°W) can be
76 divided into four general bathymetric zones: bank-top (~0–60 mbsl), upper-slope (~60–
77 250 mbsl, 2% grade), mid-slope (250–500 mbsl, 5% grade) and toe-of-slope (500–1000
78 mbsl, 1% grade). An offbank depth transect of cores (JPC25: 494 mbsl; JPC26: 546 mbsl;
79 and JPC59: 358 mbsl) stretching from the upper-slope into the Florida Straits was
80 collected aboard the R/V *Knorr* in January 2002 CE (cruise KNR166-02). Grain size was
81 measured at ~1 cm intervals in these cores, using a Beckman-Coulter (LS13320) laser
82 particle-size analyzer. Bulk mean grain-size data from JPC25, presented in Figure 2A, is
83 archived in the GSA Data Repository¹. Existing radiocarbon chronology and
84 *Globigerinoides ruber* $\delta^{18}\text{O}$ from JPC 26 (Lynch-Stieglitz et al., 2011) was
85 stratigraphically correlated to JPC25/59 using X-ray fluorescence (ITRAX) $\ln(\text{Ca}/\text{Fe})$,
86 defining the YD and EH boundaries in each core (Fig. DR1). We note, however, that this
87 approach is not aimed at differentiating events occurring in rapid succession and/or short-
88 term changes in local sedimentation rate within the YD or EH.

89 We also analyzed environmental conditions known to favor TC development and
90 intensification in two segments of the Transient Climate Evolution Experiment (TraCE),
91 a globally coupled ocean-atmosphere-land model simulation performed with Community

92 Climate System Model version 3.0 (CCSM3) (e.g., Liu et al., 2009). TraCE captures
93 much of the YD SST cooling seen in comparable North Atlantic proxy reconstructions
94 (see Table DR1). We computed TC potential intensity, absolute vorticity, and
95 tropospheric wind shear, which is a measure of tropospheric saturation deficits (see the
96 Data Repository). These metrics can be combined into a genesis potential index (Korty et
97 al., 2012), which measures the combined effects of wind shear, moist thermodynamics,
98 and convection in producing favorable conditions for tropical cyclones to form and
99 intensify. We calculated these variables using monthly TraCE output spanning the middle
100 of the YD (12.5–12.0 k.y. B.P.), during which the North Atlantic was subject to
101 freshwater hosing, and during a later 600-yr segment (10.8–10.2 k.y. B.P.) following
102 establishment of reduced EH meltwater fluxes. Genesis potential was calculated for each
103 month and then summed over June to November of each year; the seasonal totals were
104 averaged over both the YD and EH segments.

105 **RESULTS AND DISCUSSION**

106 A matrix composed largely of carbonate mud and trace quantities of iron-bearing
107 fines supports coarser-grained biogenic grains in JPC25/26/59. Despite relatively uniform
108 composition, downcore changes in color and iron abundance versus calcium-rich
109 sediments derived from the bank top (Fig. DR1), define tie-points between cores
110 coincident with deglacial flooding of the bank-top (~13 k.y. B.P.), the YD/EH transition
111 (~11.7 k.y. B.P.) and platform submergence (~10 k.y. B.P.). In general, the sediments
112 appear largely structureless, however, evidence of low-density turbidite deposition such
113 as parallel lamina (mm-scale) and sand lenses occur sporadically. Burrows, avoided
114 during sampling, were also occasionally identified by visible changes in sediment

115 structure and/or color. The $>63\ \mu\text{m}$ sediment fraction is dominated by benthic
116 foraminifera (primarily miliolids and rotalids), planktonic foraminifera, and occasional
117 pelycopod shell fragments. While we caution that no benthic foraminifera diagnostic of
118 shallow-water origin were observed in the coarsest layers, most of the pelycopod shells
119 were fractured and angular suggesting their taphonomic history included breakage during
120 transport from elsewhere.

121 We propose that the most likely mechanism for emplacement of coarse-grained
122 material in these cores is entrainment of sediment on the banktop and deposition offshore
123 by turbidites during storms. Grain-size increases downslope (Fig. DR2) and the coarsest
124 beds are poorly sorted relative to background sediments—observations that are
125 inconsistent with winnowing by the Florida Current. Preferential contourite formation
126 during the YD is also unlikely given evidence for greatly reduced AMOC strength at this
127 time (Lynch-Stieglitz et al., 2011; McManus et al., 2004; Fig. 2). Extensive seismic
128 surveying of the southwest Florida margin by Brooks and Holmes (1989) shows
129 depositional units are oriented offbank, not along the path of the Florida Current. We also
130 note higher sedimentation rates during the YD than the ensuing EH, suggesting coarse-
131 grained beds in the YD unit are net-depositional rather than erosional. General agreement
132 between grain-size records from JPC25/26 and JPC59, the latter located $\sim 15\ \text{km}$ west
133 along-bank, likely excludes local mass wasting as a viable alternative mechanism for
134 emplacement of coarser-grained units. These sites face no known active margins likely to
135 produce frequent, large, tsunamis nor do they occupy the type of steep continental margin
136 thought to be susceptible to slope failures triggered by distant earthquakes (Johnson et al.,
137 2017). While comparable TC records do not currently exist with which to definitively

138 rule out other local sediment transport mechanisms, given (1) little evidence for
139 contourite formation or tsunami-triggered mass wasting, (2) widespread observations of
140 sediment entrainment on continental shelves during modern storms (Shanmugam, 2008)
141 and (3) sedimentary evidence of density current deposition offbank the Bahamas from
142 historic major hurricanes (Toomey et al., 2013), we argue coarse-grained material in
143 cores JPC25/26/59 is largely derived from storm-triggered turbidites.

144 Grain-size variability in our cores suggests relatively more frequent high-energy
145 events during the YD with an abrupt transition to finer grained deposition moving into
146 the EH (Fig. 2A; Fig. DR2). For instance, mean grain-size in JPC 25 is $23 \pm 4 \mu\text{m}$
147 through the YD but drops to $19 \pm 2 \mu\text{m}$ during the EH section (11.7–10.2 k.y. BP).
148 Transgressive drowning of Florida Bank during Meltwater Pulse 1B (MWP1B), ~11.4–
149 11.1 k.y. B.P., limiting entrainment of sediment by storm waves, could provide another
150 explanation for the lack of coarse-grained deposits during the EH; however, recent
151 drilling of drowned reefs offshore Tahiti (Bard et al., 2010, and references therein)
152 indicates a relatively gradual change in the rate of sea-level rise from the YD (~8 mm/yr)
153 to the EH (12 mm/yr), calling into question the existence of MWP1B. Instead, we
154 propose below that sustained AMOC reduction during the YD (McManus et al., 2004)
155 produced environmental conditions that were more hostile to storms across much of the
156 tropical North Atlantic, but locally more favorable near the southeastern U.S.

157 The spatial pattern of changes in potential intensity (PI) during the YD (Fig. DR3)
158 shows that it was much lower where SSTs fell most dramatically across low latitudes of
159 the tropical Atlantic, but PI was little changed or sometimes higher where SSTs were
160 warmer relative to the remainder of the basin. Near Florida, the seasonal (June–

161 November) max PI remained high enough to support Category 5 storms throughout the
162 YD and EH (Fig. 3C; YD = 70 m s^{-1} , EH = 74 m s^{-1}). Vecchi and Soden (2007) showed
163 that PI is strongly related to relative SST rather than to absolute SST: PI is the highest
164 where waters are locally warmer than the regional average. On average, storm season
165 wind shear was higher during the YD than EH across the tropical Atlantic (Fig. DR3), but
166 lower near Florida ($\Delta = -0.3 \text{ m s}^{-1}$) and in the subtropics. In colder atmospheres, a
167 smaller quantity of water vapor is required to saturate an air column. This, in combination
168 with lower shear, yields higher genesis potential (GP in Fig. 3B) with conditions more
169 favorable for tropical cyclones near the Dry Tortugas, outweighing lower absolute local
170 SST (TraCE: YD = $25 \text{ }^\circ\text{C}$, EH = $26 \text{ }^\circ\text{C}$, comparable to Mg/Ca proxy SST from JPC26;
171 Schmidt and Lynch-Stieglitz, 2011).

172 In addition to the potential for increased storm activity in the western sub-tropics,
173 genesis potential appears largely unchanged (YD versus EH) in the southern Caribbean
174 (Fig. 3B)—the source region for most major storms tracking near the Dry Tortugas today.
175 Since 1848 CE, 11 of the 12 storms passing the JPC25 core site ($\leq 65 \text{ km}$ radius) as major
176 hurricanes (\geq Category 3) formed within or proximal to the Caribbean Sea (Fig. 1A,
177 Knapp et al., 2010), often steered by late season westerlies north/northwest over deep,
178 warm, waters on their way toward Florida. A more southerly mean position of the ITCZ
179 (Haug et al., 2001) and westerlies during the YD could have shifted hurricane tracks
180 toward Florida in late summer when warm Caribbean waters often reach their maximum
181 extent.

182 Coarse discretization of the TraCE ocean domain (25 vertical levels and ~ 200 –
183 400 km horizontal resolution at these latitudes), however, may limit its sensitivity to

184 thermocline structure and therefore sub-surface warming during episodes of sustained
185 AMOC reduction and/or migrations of the Florida Current itself (~100 km wide)—which
186 may have further augmented favorable TC conditions near our site. Tropical North
187 Atlantic sub-surface temperature is thought to be anti-correlated with AMOC strength
188 (Zhang, 2007) and Mg/Ca temperature estimates from southern Caribbean indicate
189 substantial warming (~3-4 °C) at intermediate depths during the YD (Schmidt et al.,
190 2012). Entrainment of cold water from the thermocline into the surface mixed layer by
191 hurricane-force winds brings colder water to the surface, working as a negative feedback
192 on storm intensity by reducing the transfer of heat to the atmosphere (e.g., Price, 1981).
193 In turn, however, increased hurricane mixing is thought to enhance poleward heat flux
194 (Emanuel, 2001) and, potentially, could have acted as negative feedback on YD high-
195 latitude cooling.

196 **CONCLUSIONS**

197 Despite cooler local surface temperatures, reconstructed hurricane strikes and
198 GCM experiments suggest relatively strong storm activity along the coast of Florida
199 during the Younger Dryas. While YD conditions for tropical cyclone development appear
200 unfavorable across much of the North Atlantic, the large-scale environment was more
201 conducive for TC genesis and intensification near the southeastern U.S. coast, where SST
202 cooling was less than elsewhere in the basin. Subsurface warming may also have
203 contributed to strong hurricane development near the Dry Tortugas during the YD,
204 motivating future modeling experiments that can better resolve changes in thermocline
205 depth. Complementary storm records along the Eastern Seaboard are also needed to
206 isolate the impact of deglacial sea-level rise on site sensitivity and establish whether

207 increased western North Atlantic hurricane activity is a robust feature of other
208 Pleistocene cold events (i.e., Heinrich) or, possibly, periods of slower AMOC regimes in
209 general.

210 **ACKNOWLEDGMENTS**

211 This work was supported by the U. S. Geological Survey Climate and Land Use
212 Change Research and Development Program (Toomey), the Woods Hole Oceanographic
213 Institution Ocean and Climate Change Institute (Toomey) and National Science
214 Foundation grants (OCE-1356708 to Donnelly; 1356509 to van Hengstum). Additional
215 technical support was provided by S. Madsen, R. Sullivan, and E. Roosen. We also thank
216 T. Cronin, M. Robinson, and three anonymous reviewers for their helpful feedback on
217 earlier versions of this manuscript. Any use of trade, firm, or product names is for
218 descriptive purposes only and does not imply endorsement by the U.S. Government.

219 **REFERENCES CITED**

220 Bard, E., Hamelin, B., and Delanghe-Sabatier, D., 2010, Deglacial meltwater pulse 1B
221 and Younger Dryas sea levels revisited with boreholes at Tahiti: *Science*, v. 327,
222 p. 1235–1237, doi:<https://doi.org/10.1126/science.1180557>.

223 Brooks, G.R., and Holmes, C.W., 1989, Recent carbonate slope sediments and
224 sedimentary processes bordering a non-rimmed platform: southwest Florida
225 continental margin, *in* Crevello, P.D., et al., eds., *Controls on Platform and Basin
226 Development: Society of Economic Paleontologists and Mineralogists Special
227 Publication 44*, p. 259–272, doi:<https://doi.org/10.2110/pec.89.44.0259>.

228 Clark, P.U., Marshall, S.J., Clarke, G.K., Hostetler, S.W., Licciardi, J.M., and Teller, J.T.,
229 2001, Freshwater forcing of abrupt climate change during the last glaciation:
230 Science, v. 293, p. 283–287, <https://doi.org/10.1126/science.1062517>.

231 Donnelly, J.P., Roll, S., Wengren, M., Butler, J., Lederer, R., and Webb, T., 2001,
232 Sedimentary evidence of intense hurricane strikes from New Jersey: *Geology*, v. 29,
233 p. 615–618, doi:[https://doi.org/10.1130/0091-](https://doi.org/10.1130/0091-7613(2001)029<0615:SEOIHS>2.0.CO;2)
234 [7613\(2001\)029<0615:SEOIHS>2.0.CO;2](https://doi.org/10.1130/0091-7613(2001)029<0615:SEOIHS>2.0.CO;2).

235 Emanuel, K., 2001, Contribution of tropical cyclones to meridional heat transport by the
236 oceans: *Journal of Geophysical Research, D, Atmospheres*, v. 106, D14, p. 14771–
237 14781, <https://doi.org/10.1029/2000JD900641>.

238 Haug, G.H., Hughen, K.A., Sigman, D.M., Peterson, L.C., and Röhl, U., 2001,
239 Southward migration of the Intertropical Convergence Zone through the Holocene:
240 Science, v. 293, p. 1304–1308, doi:<https://doi.org/10.1126/science.1059725>.

241 Johnson, H.P., Gomberg, J.S., Hautala, S.L., and Salmi, M.S., 2017, Sediment gravity
242 flows triggered by remotely generated earthquake waves: *Journal of Geophysical*
243 *Research: Solid Earth*, v. 122, doi:<https://doi.org/10.1002/2016JB013689>.

244 Knapp, K.R., Kruk, M.C., Levinson, D.H., Diamond, H.J., and Neumann, C.J., 2010, The
245 International Best Track Archive for Climate Stewardship (IBTrACS): *Bulletin of*
246 *the American Meteorological Society*, v. 91, p. 363–376,
247 doi:<https://doi.org/10.1175/2009BAMS2755.1>.

248 Korty, R.L., Camargo, S.J., and Galewsky, J., 2012, Tropical cyclone genesis factors in
249 simulations of the Last Glacial Maximum: *Journal of Climate*, v. 25, p. 4348–4365,
250 doi:<https://doi.org/10.1175/JCLI-D-11-00517.1>.

251 Kossin, J.P., 2017, Hurricane intensification along United States coast suppressed during
252 active hurricane periods: *Nature*, v. 541, p. 390–393,
253 doi:<https://doi.org/10.1038/nature20783>.

254 Liu, Z., Otto-Bliesner, B., He, F., Brady, E., Tomas, R., Clark, P., Carlson, A., Lynch-
255 Stieglitz, J., Curry, W., and Brook, E., 2009, Transient simulation of last deglaciation
256 with a new mechanism for Bølling-Allerød warming: *Science*, v. 325, p. 310–314,
257 doi:<https://doi.org/10.1126/science.1171041>.

258 Lynch-Stieglitz, J., Schmidt, M.W., and Curry, W.B., 2011, Evidence from the Florida
259 Straits for Younger Dryas ocean circulation changes: *Paleoceanography*, v. 26,
260 p. PA1205, doi:<https://doi.org/10.1029/2010PA002032>.

261 McManus, J., Francois, R., Gherardi, J.-M., Keigwin, L., and Brown-Leger, S., 2004,
262 Collapse and rapid resumption of Atlantic meridional circulation linked to deglacial
263 climate changes: *Nature*, v. 428, p. 834–837,
264 doi:<https://doi.org/10.1038/nature02494>.

265 Price, J.F., 1981, Upper ocean response to a hurricane: *Journal of Physical*
266 *Oceanography*, v. 11, p. 153–175, doi:[https://doi.org/10.1175/1520-0485\(1981\)011<0153:UORTAH>2.0.CO;2](https://doi.org/10.1175/1520-0485(1981)011<0153:UORTAH>2.0.CO;2).

268 Schmidt, M.W., Chang, P., Hertzberg, J.E., Them, T.R., Ji, L., and Otto-Bliesner, B.L.,
269 2012, Impact of abrupt deglacial climate change on tropical Atlantic subsurface
270 temperatures: *Proceedings of the National Academy of Sciences of the United States*
271 *of America*, v. 109, p. 14348–14352, doi: <https://doi.org/10.1073/pnas.1207806109>
272 (erratum available at <https://doi.org/10.1073/pnas.1216897109>).

273 Schmidt, M.W., and Lynch-Stieglitz, J., 2011, Florida Straits deglacial temperature and
274 salinity change: Implications for tropical hydrologic cycle variability during the
275 Younger Dryas: *Paleoceanography*, v. 26, PA4205,
276 doi:<https://doi.org/10.1029/2011PA002157>.

277 Shanmugam, G., 2008, The constructive functions of tropical cyclones and tsunamis on
278 deep-water sand deposition during sea level highstand: Implications for petroleum
279 exploration: *The American Association of Petroleum Geologists Bulletin*, v. 92,
280 p. 443–471, doi:<https://doi.org/10.1306/12270707101>.

281 Sobel, A.H., Camargo, S.J., Hall, T.M., Lee, C.-Y., Tippett, M.K., and Wing, A.A., 2016,
282 Human influence on tropical cyclone intensity: *Science*, v. 353, p. 242–246,
283 <https://doi.org/10.1126/science.aaf6574>.

284 Toomey, M.R., Curry, W.B., Donnelly, J.P., and van Hengstum, P.J., 2013,
285 Reconstructing 7000 years of North Atlantic hurricane variability using deep-sea
286 sediment cores from the western Great Bahama Bank: *Paleoceanography*, v. 28,
287 p. 31–41, doi:<https://doi.org/10.1002/palo.20012>.

288 Vecchi, G.A., and Soden, B.J., 2007, Effect of remote sea surface temperature change on
289 tropical cyclone potential intensity: *Nature*, v. 450, p. 1066–1070,
290 doi:<https://doi.org/10.1038/nature06423>.

291 Zhang, R., 2007, Anticorrelated multidecadal variations between surface and subsurface
292 tropical North Atlantic: *Geophysical Research Letters*, v. 34, L12713,
293 doi:<https://doi.org/10.1029/2007GL030225>.

294 **FIGURE CAPTIONS**

295 Figure 1. Site maps. A: Historic North Atlantic hurricane tracks passing within 65 nm of
296 our site at major hurricane strength (96 kts, 1 min maximum sustained wind [MSW])
297 since 1848 CE (Knapp et al., 2010). White circle pinpoints the Dry Tortugas, abbreviated
298 DT. Location used in Figure 2 proxy reconstructions by dots: red—Vema 12–107 (VM);
299 yellow—Bermuda Rise (BR); light gray—Barbados (BB); dark gray—Cariaco Basin
300 (CB). Tracks noted of major hurricanes that formed in the Caribbean (dark gray) versus
301 one from the eastern North Atlantic (light gray). Background color map was compiled
302 from National Oceanic and Atmospheric Administration (NOAA) monthly satellite-
303 derived ocean heat content data for the 2013–2015 CE storm seasons (Data Repository
304 [see footnote 1]). B: Regional map of southern Florida, northern Caribbean, and Gulf of
305 Mexico. Red arrow shows the generalized path of the Yucatan (YC), Loop and Florida
306 Currents (FC). Location of transect shown in inset C is given by black line from DT to c.
307 Bahamas hurricane reconstruction sites from Toomey et al. (2013) indicated by triangle.
308 Blue shading indicates shallow water areas (<120 mbsl). C: Schematic profile across
309 offbank core transect. Jumbo piston core (JPC) 59 is located ~15 km west of JPC25/26
310 and projected into line DT-c. Maps were created using Matlab[®] m_map function suite
311 written by Rich Pawlowicz (University of British Columbia).

312

313 Figure 2. Climatic variability across the Younger Dryas/ early Holocene (YD/EH)
314 transition. A: Grain-size record from Florida Straits core KNR166–2 JPC25. Raw data
315 are shown in gray with 50-yr moving average filtered time-series given by blue line. Note
316 broken y-axis. B: Mg/Ca paleo-temperature proxy data (red) from core VM12–107
317 (Schmidt et al., 2012). C: Bermuda Rise (core OCE326-GGC5) ²³¹Pa/²³⁰Th record of

318 Atlantic Meridional Overturning Circulation (AMOC) (McManus et al., 2004) (yellow).
319 D: Subsidence corrected relative sea-level records from Barbados (gray) and Tahiti (light
320 blue) adapted from Bard et al. (2010, and references therein). E: Cariaco Basin,
321 Venezuela (Ocean Drilling Program [ODP] Site 1002), %Ti (Haug et al., 2001) (dark
322 gray). Blue and pink shading highlights early Holocene (EH) and Younger Dryas (YD)
323 Transient Climate Evolution Experiment (TraCE) segments, respectively.

324

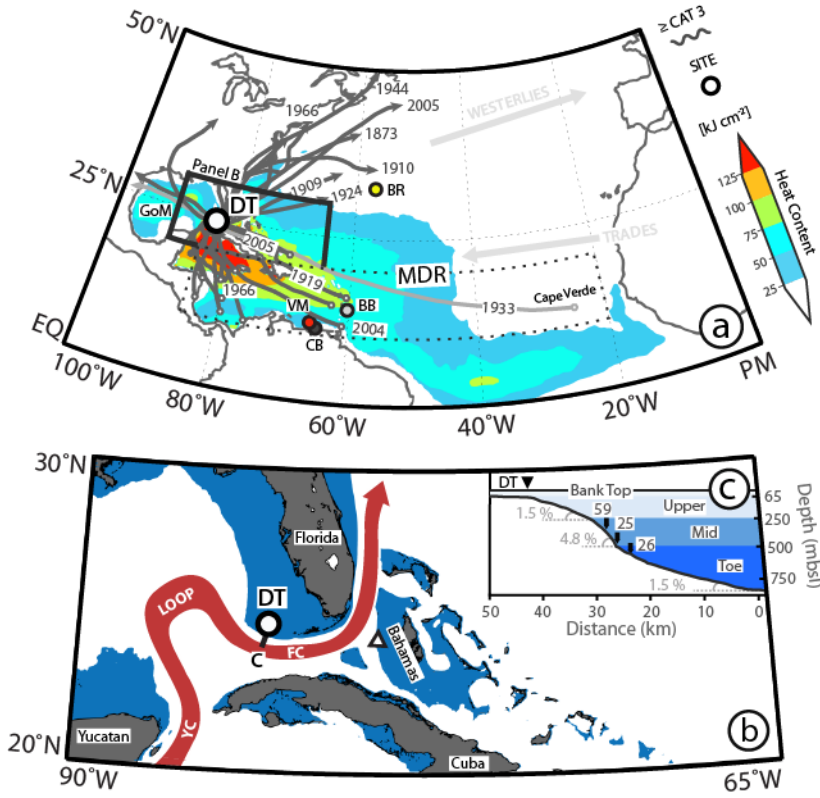
325 Figure 3. Simulated changes in climatic controls on hurricane activity between the
326 Younger Dryas (YD, 12.0–12.5 k.y. B.P.) and early Holocene (EH, 10.2–10.8 k.y. B.P.).
327 Spatial difference in storm season (A) surface temperature and (B) genesis potential
328 index (GPI), averaged for each Transient Climate Evolution Experiment (TraCE)
329 interval. C: Filtered (20 yr) time series of maximum potential intensity near the Dry
330 Tortugas (red) and Barbados (gray) from 13,850 yr B.P. through the EH.

331

332 ¹GSA Data Repository item 2017xxx, grain-size data, is available online at
333 <http://www.geosociety.org/datarepository/2017/> or on request from
334 editing@geosociety.org.

335

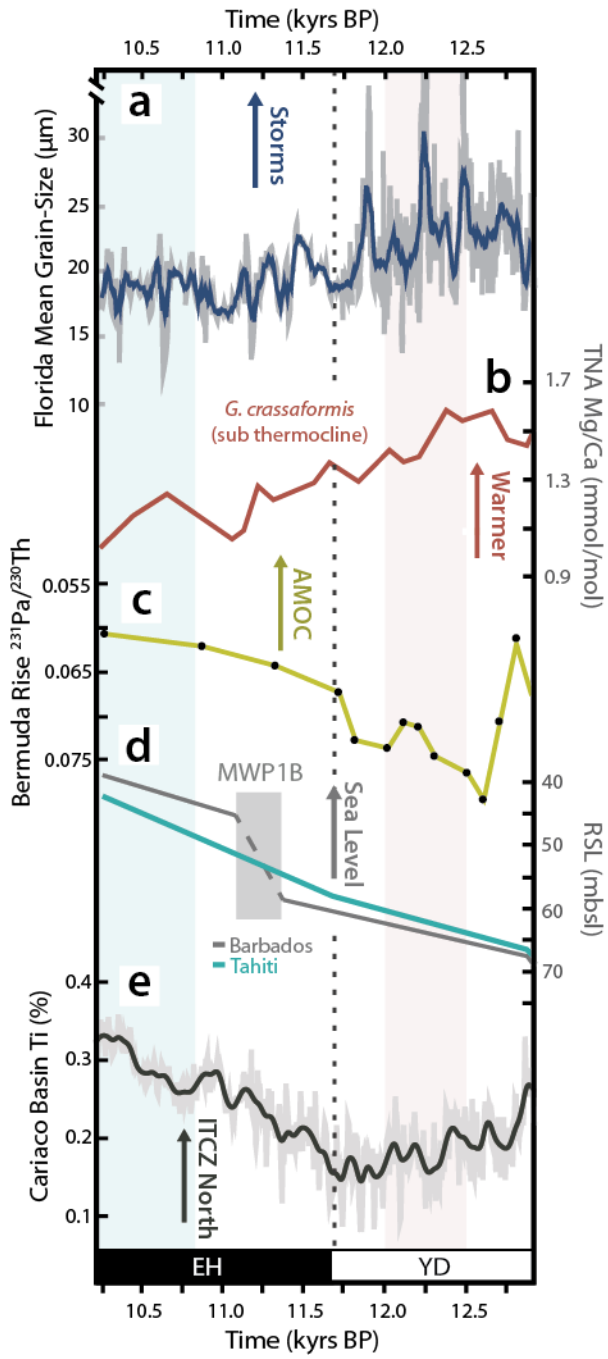
336 Figure 1:



337

338

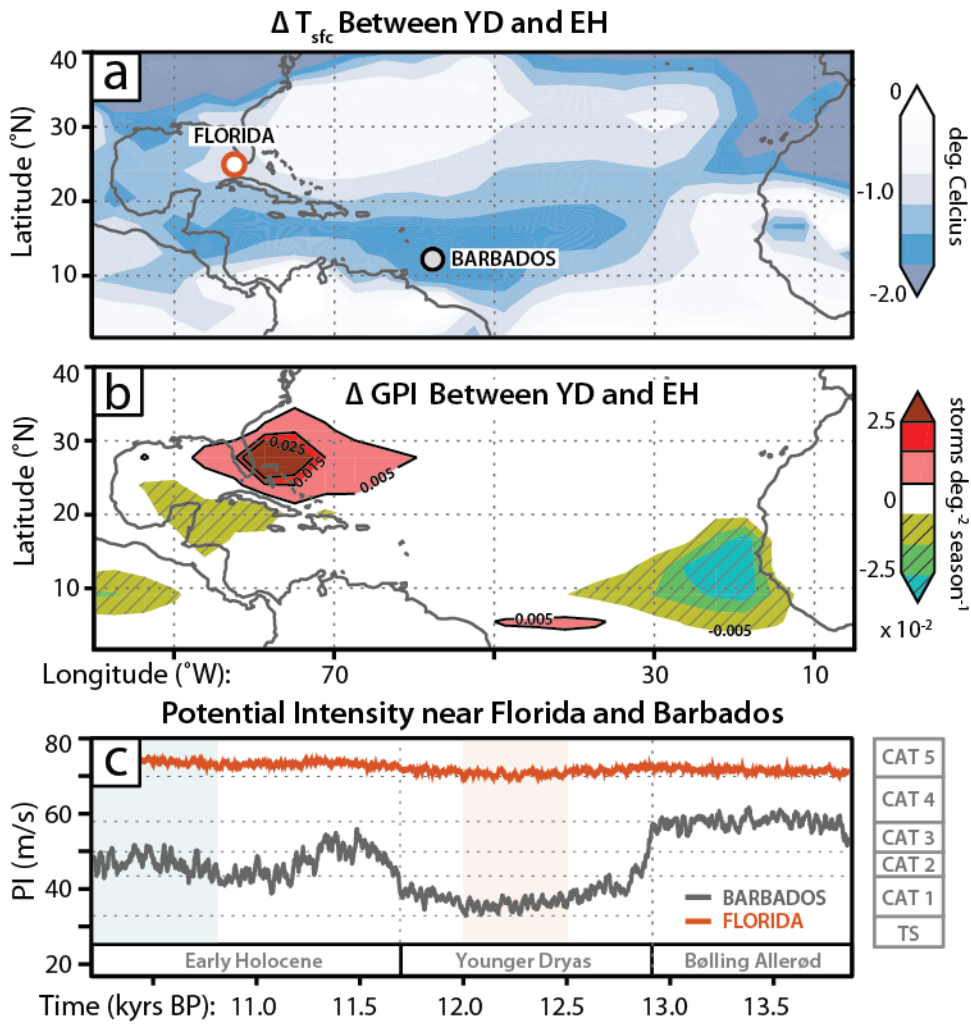
339 Figure 2:



340

341

342 Figure 3:



343